Intraseasonal and low frequency processes contributing to the December 2013 heat wave in Southern South America

Mariano S. Alvarez[1,2,3] · Bibiana Cerne[1,2,3] · Marisol Osman[1,2,3] · Carolina S. Vera[1,2,3]

Abstract

In the second fortnight of December 2013, the longest heat wave registered until then occurred in Buenos Aires city and over a large region of Argentina, with large socio-economic impacts. Excess heat indexes were used to characterize this heat wave, which occurred within the warm season with largest number of heat wave days. This extreme event resulted in the longest consecutive period of heat wave conditions between 1979 and 2014. This event was the result of the combined activity of short intraseasonal (10–30 days), long intraseasonal (30–90 days) and larger (more than 90 days) time scales. Accounting for the lower frequency, dry soil moisture anomalies were observed in Argentina during autumn, winter and spring of 2013 probably favoring more extreme values in the temperature anomalies. Weekly geopotential heights anomalies computed during the event showed that the combination of the negative phase of the Southern Annular Mode and a wave-4 pattern at midlatitudes favored the development of positive geopotential height anomalies over southern South America which promoted subsidence motions there. Intraseasonal variability played a key role in the persistence of the heat wave. The development of an MJO event over the Indian Ocean (RMM phase 3) 12 days prior to the beginning of the heat wave may have contributed to organize the extratropical wave train which in turn favored the anticyclonic upper-level anomaly development over southern South America. Furthermore, an intense SACZ event during the first 12 days of the heat wave favored clear-sky conditions and diabatic heating as well as subsidence, while during the last days it was the northerly advection of warmer air in the 10–30-day time scale that maintained the intensity of the temperature anomalies.

Keywords Heat wave · Intraseasonal variability · Soil moisture · South America

1 Introduction

The analysis and prediction of intense heat waves over southern South America are important as they affect a large number of people, infrastructure and ecosystems (Campetella and Rusticucci 1998; Alessandro and de Garín 2003; Leva et al. 2005; García-Herrera et al. 2010; Bastos et al. 2014; Geirinhas et al. 2019). These events produce dangerous levels of thermal stress in the population specially when they are very persistent, as the event that occurred during the second half of December 2013, which was cataloged by the Argentinian National Weather Service (SMN, its acronym in Spanish) as an event of heat wave (SMN 2014). The reported mortality related to this event showed an increase of 50% of the deceases (irrespectively of their cause) respect to the summer mean (Almeira et al. 2016). The persistent high values of temperature also produced a strong impact on electricity consumption, showing an increase of 22.6% respect to the previous month. In fact, part of the largest urban area of Argentina was affected by a prolonged power outage which increased the stress over the population. This heat event also affected Uruguay, where it favored the development of a wildfire in the Department of Rocha affecting about 50 ha of forest.

✉ Mariano S. Alvarez
    alvarez@cima.fcen.uba.ar

1   Departamento de Ciencias de la Atmósfera y los Océanos, Facultad de Ciencias Exactas y Naturales (DCAO/FCEN), Universidad de Buenos Aires (UBA), Buenos Aires, Argentina

2   Centro de Investigaciones del Mar y la Atmósfera (CIMA), Universidad de Buenos Aires-Consejo Nacional de Investigaciones Científicas y Técnicas (UBA-CONICET), Buenos Aires, Argentina

3   Institut Franco-Argentin d'Estudes sur le Climat et ses Impacts, Unité Mixte Internationale (UMI-IFAECI/CNRS-CONICET-UBA), Buenos Aires, Argentina

The extraordinary impact of the heatwave in the population was not only due to high temperatures but also to its persistence and intensity, considering the accumulation of degrees over thresholds (Barros et al. 2015). Since December 11th, the temperature began to rise in the central region of Argentina. A week later, high temperatures intensified, and the affected region was extended northward (SMN 2014). Maximum and/or minimum temperatures surpassed the 90th percentile (1961–1990) between 5 and 18 days (SMN 2014) in many meteorological stations located in the area affected by this heat wave, becoming climatological records for some of them.

It becomes evident that the heat wave persistence may be indicating that the natural variability on intraseasonal timescales could have played a key role. Previous works (Cerne et al. 2007; Cerne and Vera 2011) show that the dynamics associated with intraseasonal variability has a major influence on the development of persistent summer heat waves. Such influence is related in most cases with the activity of the South Atlantic Convergence Zone (SACZ).

The most distinctive feature of summer variability on intraseasonal timescales over South America, as depicted from OLR or precipitation anomalies, is a dipolar pattern (Nogues-Paegle and Mo 1997 and the references therein). The dipole has centers of action of opposite sign in both SACZ and southeastern South America (SESA), regions approximately located as marked in Fig. 1. The phase with enhanced precipitation over the SACZ promotes subsidence conditions over SESA, favoring the development of an anticyclonic circulation there, which in turn results in a temperature rise under relatively dry conditions (Cerne and Vera 2011). In the opposite phase, enhanced precipitation over SESA is observed as well as a cyclonic anomaly at the tropics, that usually promotes the intensification of the South America low level jet (LLJ) (Nogues-Paegle and Mo 1997). Moreover, the summer dipole pattern presents two main bands of temporal variability with periods between 10–30 days (hereafter, Short Intraseasonal Band, SIB), and 30– 90 days (hereafter, Long Intraseasonal Band, LIB), each band influenced by different large scale forcings (Gonzalez and Vera 2014; Vera et al. 2018). The LIB is related to an eastward traveling wavenumber-1 structure in OLR and circulation anomalies in the tropics, similar to that associated to the Madden and Julian Oscillation (MJO, e.g., Madden and Julian 1994). The LIB is also related to a quasi-stationary teleconnection pattern extended along the South Pacific Ocean linking Australia with South America (Vera et al. 2018). The SIB is associated with Rossby-like wave-trains extended along the south Pacific and influencing South America too, although it does not seem to be associated with the activity of propagating tropical convection. There are some evidences that the convergence zones at the subtropics (e.g. SPCZ, SACZ) might play a role in SIB activity,
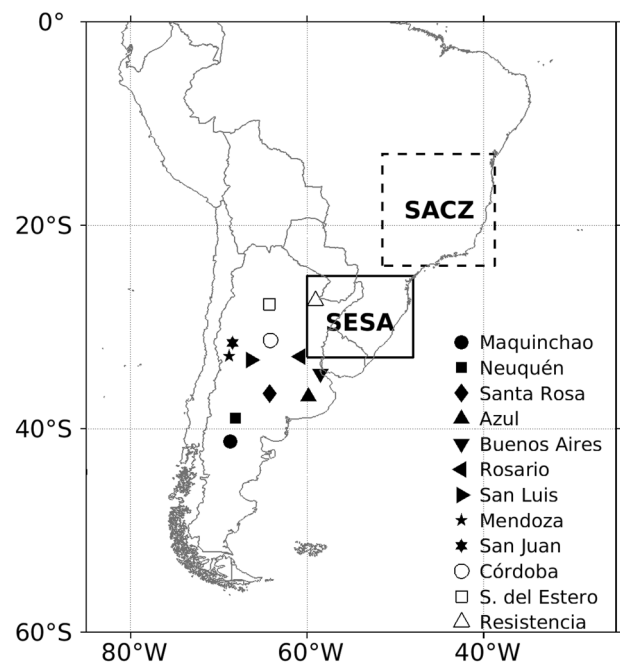

Fig. 1 Localization of the SACZ and SESA regions in South America (see text for details) and location of the weather stations of Argentina used in the analysis of Table 1

however, its source is not completely clear yet (Gonzalez and Vera 2014).

Besides the contribution of atmospheric dynamics to the development of heat waves, some authors claimed that soil land surface processes may also contribute significantly, in combination with circulation patterns, in the occurrence of heat waves and the magnitude of the temperature anomalies. In particular, Fischer et al. (2007b) showed that for the extreme heat wave of 2003 in Europe, the negative soil moisture anomalies that persisted for many months before the event strongly reduced latent cooling and therefore intensified the surface temperature anomalies, amplifying the induced heat-stress conditions. In addition, land-atmosphere interactions can contribute in a major extent to the duration and spatial extension of heat waves, as was concluded by Fischer et al. (2007a) using numerical simulations. These findings for heat waves over Europe motivate the analysis of the evolution of soil moisture anomalies during the seasons previous to the event to evaluate its contribution to the temperature anomalies observed. This might be particularly relevant over La Plata Basin where the coupling strength between soil moisture, evapotranspiration and temperature shows a hot spot (Ruscica et al. 2015).

Therefore, the aim of this paper is to verify the influence of the intraseasonal variability, considering the 10–30 and 30–90 timescales separately, over South America in the occurrence of this event and to explore the possible remote and local factors that might have favored its persistence. In

addition, the possible mechanisms acting in longer time scales are also examined. This paper is organized as follows: Sect. 2 describes the data and methodologies used, Sect. 3 presents the results, where the heat wave period is first characterized and then the instraseasonal and low frequency forcings are analyzed. Finally, a discussion is presented in Sect. 4.

2 Data and methodology

The determination of the heatwave event was done using the maximum daily temperature (Tmax) and minimum daily temperature (Tmin) and the mean daily temperature (T), computed as the mean between Tmax and Tmin. Such determination was made based on the daily Tmax and Tmin data measured in Buenos Aires station (87585) of the SMN between 1979 and 2014, along with other SMN stations in the study region (Table 1).

There are several ways of defining a heat wave, which were revised in Perkins and Alexander (2013) and Perkins et al. (2015). On the one hand, the amount of days in which the temperature exceeds a certain threshold can be used to determine a heat wave. The selected thresholds in this work for the Tmin and Tmax are the CTN90pct and CTX90pct, which are defined as the calendar day 90th percentile of Tmin and Tmax respectively, based on a 15-day window. These relative thresholds are useful as they consider the seasonal cycle of the temperature, therefore allowing comparisons against heat waves that occur in different months across the warm season. On the other hand, a heat wave can be defined when an index fulfills certain criteria. The Excess Heat Indexes are defined as following:

$$EHI(accl.) = [(T_i + T_{i-1} + T_{i-2})/3] \\ - [(T_{i-3} + \cdots + T_{i-32})/30],$$
$$EHI(sig.) = [(T_i + T_{i-1} + T_{i-2})/3] - T90_i,$$

where T_i is the average daily temperature for day i and $T90_i$ is the calendar day 90th percentile of T based on a 15-day window. The EHI(accl.) is defined as the difference between the temperatures averaged over a window of 3 days minus the mean over the preceding 30 days, which accounts for acclimatization. The EHI(accl.) is particularly important to consider when relating heat-stress conditions with high mortality, which might not only be related to extreme temperatures but also to hot periods that strike after consecutive days characterized by cooler conditions. The EHI(sig.) accounts for the difference of the 3-day averaged temperature respect to a climatological extreme threshold, and gives a measure of statistical significance. When combined, the EHI result in the Excess Heat Factor (EHF) as follows:

$$EHF = max[1, EHI(accl.)] * EHI(sig.)$$

and positive values of EHF define heatwave-like conditions for day i. Additionally, the seasonal sum of participating heat wave days (HWF), the length of the longest event of the season (HWD) and the largest EHF of the season (HWA) were computed for a retrospective analysis, considering the November–March seasons within the period of study.

Daily fields of temperature at 925 hPa, zonal and meridional wind at 850 hPa and geopotential height of 300 hPa were taken from the ERA Interim database (Berrisford et al. 2011), from 1979 to 2016. Linear trend was first removed from all temporal series and afterwards, the seasonal cycle. The latter was determined through the first three harmonics of the climatological mean day for each grid point. Anomalies were then filtered using a 101-weighted Lanczos filter (Duchon 1979) retaining periods between 10 and 30 days (SIB), between 30 and 90 days (LIB) and those periods longer than 90 days (LP).

The regional intraseasonal variability was described considering the first EOF of 30–90-day filtered OLR anomalies in eastern South America (hereafter called as 3090-SIS pattern) for the October–April season. In that sense, the associated standardized principal component (hereafter called as 3090-SIS index) was considered to describe the pattern temporal evolution (Alvarez et al. 2017 and Vera et al. 2018). The 3090-SIS pattern is a dipole with centers of action in the SACZ (more intense) and SESA regions. When the 3090-SIS index is positive (negative), convection is favored (inhibited) in SESA and inhibited (favored) in the SACZ region.

The influence of soil moisture (SM) variability on extreme temperatures was assessed using the Global Land Data Assimilation System (GLDAS, Rodell et al. 2004) monthly simulations. GLDAS uses the Noah land surface model version 3.3 (Ek et al. 2003). We considered two components spanning the same period as temperature data: one forced entirely with the Princeton meteorological forcing data (hereafter, GLDAS-2.0), which goes from January 1979 to December 2010, and the other forced with a combination of model and observation-based forcing data sets (hereafter, GLDAS-2.1), which spans from January 2000 up to the present. The Standardized Soil Moisture Anomalies (SSMA) based on the root zone layer (RZ, 0–100cm) were considered to characterize moisture conditions. The work by Spennemann et al. (2015) has shown that SSMA are a useful tool to describe soil moisture anomalies over Southern South America and to develop soil moisture indexes. The SSMA are calculated for each grid point as:

$$SSMA(i,j,t) = \frac{(SM(i,j,t) - \overline{SM(i,j)})}{\sigma(SM(i,j))}$$

where t corresponds to each season (i.e. December–January–February), the overbar is the long-term average and σ is the standard deviation for the corresponding season,

respectively. Thus, for each season the corresponding seasonal mean value of that season is subtracted and then divided by its standard deviation (that represents the corresponding interannual variability). Given that the period of study is not completely covered by any of both GLDAS database, we used GLDAS-2.0 when we analyzed SSMA during the 1979–2010 period and GLDAS-2.1 for the 2010–present. An analysis of the temporal series of the SSMA of both datasets during the overlapping period for the domain of study reveals that both datasets are highly correlated and the periods of extreme dry and wet conditions match (not shown).

3 Results

3.1 Heat wave period

The time series of Tmax and Tmin for Buenos Aires during December 2013 are shown in Fig. 2a, together with the time series of CTX90pct and CTN90pct. During the first fortnight of the month, Tmax oscillated between 35 and 24°C, only surpassing the CTX90pct one day at a time. Conversely, since 13th, the Tmax was larger than CTX90pct for periods of several days, reaching a maximum of 39°C on the 26th. The minimum temperature was mostly under CTN90pct during the first fortnight of December, and from the 15th it experimented a long period above the threshold (excepting on the 21st and the 31st). This period of hot nights increased the general discomfort of the population and the higher-level alert was emitted by the SMN.

The evolution of excess heat indexes is presented in Fig. 2b. The EHI(accl.) was positive from the 13th until the end of the month, indicating that the averaged Tmed during the time periods containing the calendar day in consideration and the two previous ones, was consistently larger than the average Tmed for the previous 30 days. Also, the EHI(sig.) was positive between the 15th and 19th and 23rd and 31st, indicating that Tmed was also above the moving daily 90th percentile for several consecutive days. Therefore, the EHF resulted positive, indicating heat wave conditions in two periods: 15–19th and 23rd–31st, of 5 and 9 consecutive days respectively. Given these results, the period analyzed in the next sections spans from the 15th to the 31st of December.

A similar analysis was performed for the temperature observed at other weather stations representative of central Argentina, between 41 and 27°S, and which are marked in Fig. 1. Results are summarized in Table 1. The EHF revealed that all these stations registered heat wave conditions during December 2013, and furthermore, the EHF resulted positive for 7 or more consecutive days during December 2013 for 6 of the analyzed stations, generally with a similar number of days of Tmin and Tmax above the respective thresholds.
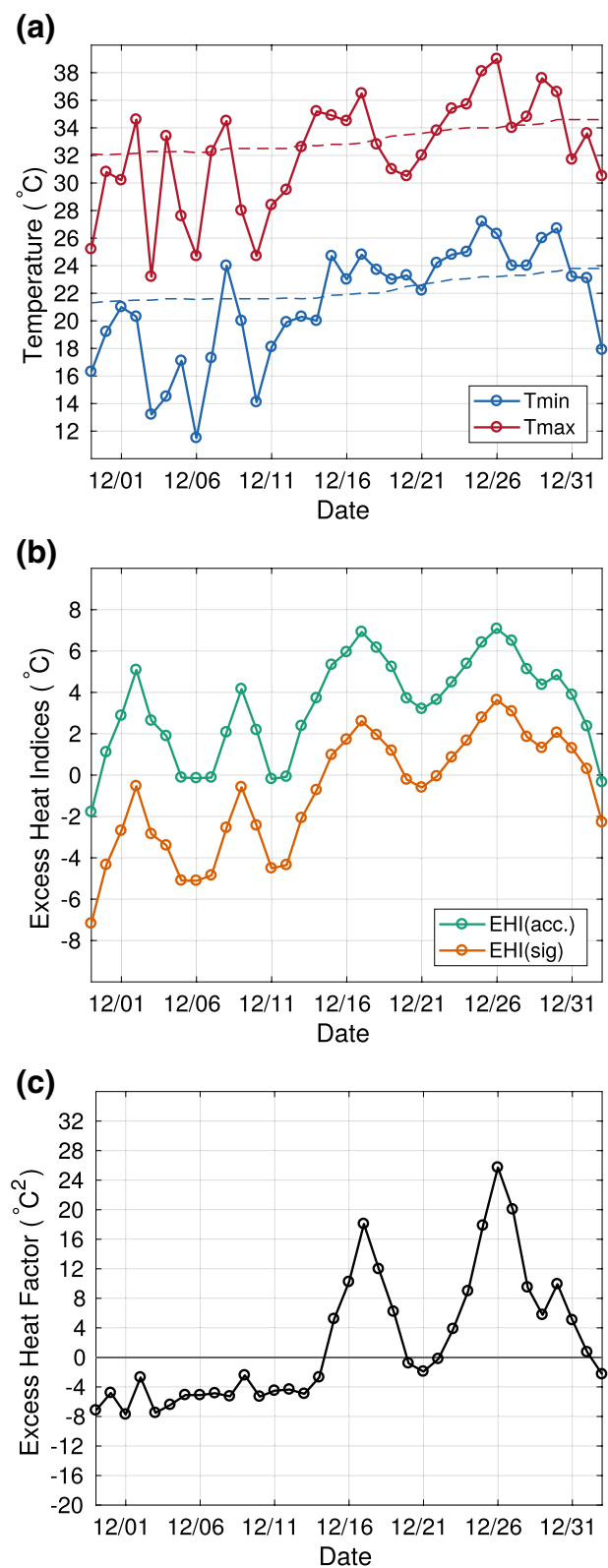

Fig. 2 For Buenos Aires, on December 2013 **a** maximum and minimum temperature (full red and blue lines respectively) along with the CTX90pct and CTN90pct thresholds (dashed red and blue lines respectively). **b** EHI(acc.) and EHI(sig.) and **c** Excess Heat Factor. See text on Sect. 2 for details

Table 1 During December 2013, for each weather station of Argentina, their latitude, longitude and number of days with: a positive Excess Heat Factor, positive EHF (considering the longest period of consecutive days), Tmin and Tmax above the CTN90pct and CTX90pct thresholds

Station			Number of days with			
Name	lat (°S)	lon (°W)	EHF > 0	Longest EHF > 0	Tmin > $CTN90pct$	Tmax > $CTX90pct$
Maquinchao	41.25	68.73	10	10	3	13
Neuquen Aero	38.95	68.13	13	11	11	11
Santa Rosa Aero	36.57	64.27	14	7	12	14
Azul Aero	36.83	59.88	9	5	8	13
Buenos Aires O.C.	34.58	58.48	14	9	16	16
Rosario Aero	32.92	60.78	14	13	13	14
San Luis Aero	33.27	66.35	5	4	10	8
Mendoza O.C.	32.88	68.85	8	5	8	8
San Juan Aero	31.57	68.42	8	5	12	6
Cordoba Aero	31.3	64.2	6	6	4	11
Santiago del Estero Aero	27.77	64.3	9	9	12	11
Resistencia Aero	27.45	59.05	5	5	6	8

The location of the weather stations is marked in Fig. 1

The latter confirms that the long heat wave event affected not only Buenos Aires city but a large region of the country.

The EHF was also analyzed retrospectively through the HWD and HWF during the austral warm season (defined as November–March) between 1979 and 2014 for Buenos Aires (Fig. 3). The heat wave under analysis occurred within the season with largest number of heat wave days (HWF), and the period accounted for the longest consecutive period of heat wave conditions (largest HWD, 10 days) in the record,. In this way, the December 2013 heat wave stands out from the record also using the EHF perspective, and it is therefore interesting to further analyze the dynamic conditions that favored its persistence. The 2008/2009 season is also noticeable, as it presents the same HWD as during the 2013/2014 season and the second largest HWF. However, the largest amplitude of the EHF for each warm season (HWA) was not achieved within neither of these two seasons: the largest maximums of EHF resulted 2012/2013 and 1995/1996, and in both the heat wave conditions started in the first week of November.

The anomaly series of T in Buenos Aires was decomposed using harmonic analysis, and the harmonics were grouped as those with periods between 10 and 30 days, 30 and 90 days and larger than 90 days. Figure 4 shows these series from 15th of November 2013 until 16th January 2014. The warm period detected before through the different indexes is clearly discernible. Also, the comparison between the full anomalies with those which account for periods longer than 10 days shows that synoptic activity (periods shorter than 10 days) did not contribute considerably to this warm event. In

Fig. 3 For Buenos Aires November–March seasons (left axis) the length of the longest season event (HWD, darker bars) and the sum of participating heat wave days in the season (HWF). The height of both bars is considered from 0. In some seasons, as 1979/1980, HWD and HWF are equal, and seasons with no HWD are not plotted. (right axis) Dots represent the maximum EHF amplitude for each season (HWA, units in $°C^2$)
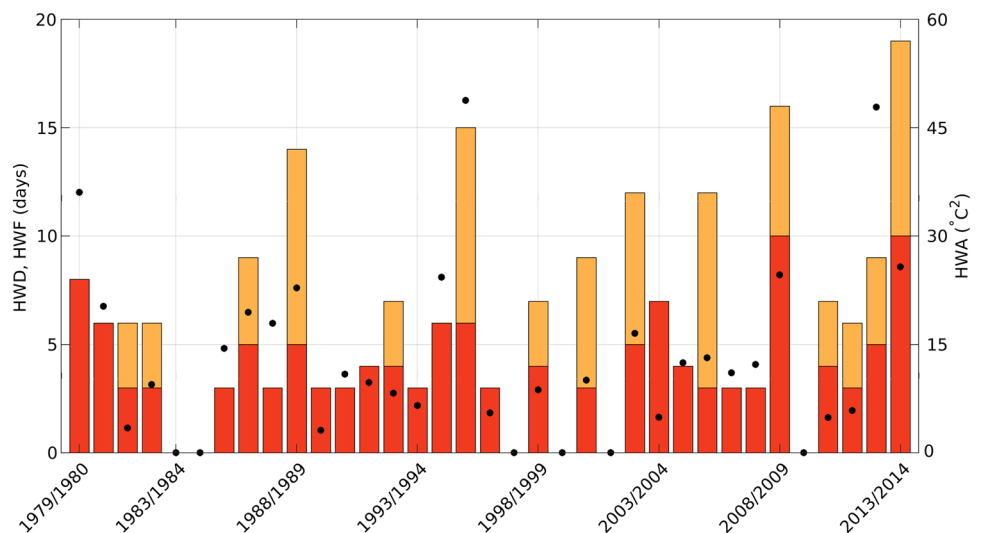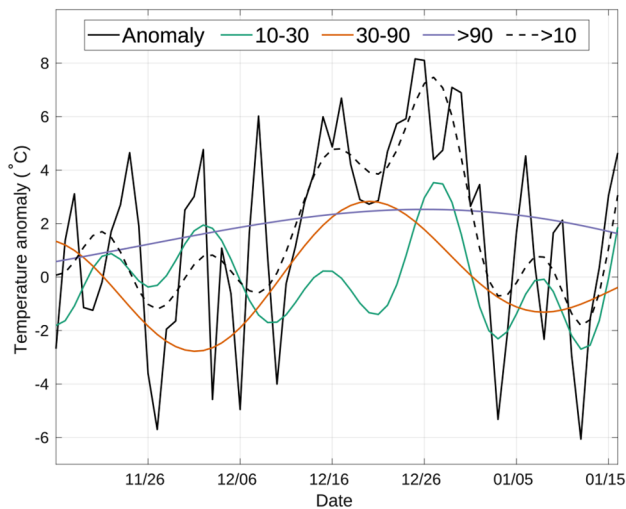
Fig. 4 For Buenos Aires, from 15th November 2013 to 16th January 2014, mean daily temperature anomaly (black line), the sum of harmonics with periods between 10 and 30 days (green line), 30 and 90 days (orange line), larger than 90 days (blue line) and larger than 10 days (dashed black line)

this way, Fig. 4 shows that the warm period extended along the second half of December was the result of the contributions of: (i) the 30–90 day variability, which exhibited a peak between the 16th and 25th, (ii) the 10–30 day variability, that presented a peak between the 25th and the 30th, and (iii) the variability of periods longer than 90 days with maximum during the second fortnight of December. It is noteworthy that when analyzed retrospectively, the variability of periods longer than 90 days of the anomaly series of T in Buenos Aires only exceeded 2°C 8 times between 1979 and 2014, being this heat wave period one of them.

The combined activity of variability associated with different temporal ranges implies that different dynamical processes might have been acting along the second fortnight of December to maintain the high temperatures over central Argentina. Therefore, the period associated with the heat wave is divided into three periods: from the 15th to the 20th, from the 21st to the 26th and 27th to 31st, which are explored in the following sections.

3.2 Intraseasonal dynamics

Composites of different atmospheric variables were computed to describe the dynamical characteristics associated with the heat wave under study. We first identify the regions where the temperature anomalies maximized in each of the intraseasonal time scales to afterwards relate them to the atmospheric circulation and the activity of modes of variability. Figure 5 then shows the temperature anomalies at

925 hPa and the corresponding SIB-filtered and LIB-filtered anomalies for each of the three periods within the heat wave.

During the first period, a large warm anomaly extended over southern South America, including central Chile, most of Argentina, Uruguay and southeastern Brazil, which reached a magnitude of above 3.75°C (Fig. 5a). The SIB contributed to the warm anomalies in northern Patagonia up to 35°S (Fig. 5b), while the LIB-filtered anomaly (Fig. 5c) influenced an area as extensive as that covered by the unfiltered anomaly (Fig. 5a). Northern Patagonia, around 40°S, was the region where the LIB-filtered anomaly values were maximized. During the next period of 6 days, the unfiltered warm anomaly was located slightly to the north and extended more into the South Atlantic Ocean, keeping, in general, its magnitude comparing to the preceding period (Fig. 5d). The SIB-filtered anomaly extended to the north over central Argentina and towards the Atlantic Ocean (Fig. 5e), while the warm LIB-filtered anomaly was located mostly over eastern Argentina, Uruguay, southern Brazil, covering the South Atlantic Ocean western branch (Fig. 5f).

During the last 5 days of the heat wave, the warm unfiltered anomaly was located to the north of 40°S, extending more pronouncedly towards south Atlantic Ocean comparing to the previous anomaly scenarios. The higher values were recorded throughout a region encompassing northern Argentina, Uruguay and Southern Brazil. (Fig. 5g). To the south, a large negative anomaly developed over the ocean. The warm anomalies related to the SIB maximized over northwestern Argentina and along the eastern coast of southeastern South America, while cold anomalies in the SIB were observed in northwestern Patagonia and central Chile and also in the southwestern Atlantic Ocean (Fig. 5h). The LIB-filtered anomaly remained in the same region respect to the previous period but with lower magnitude (Fig. 5i). The LIB also contributed during the last 5 days to a decrease in temperature over Patagonia.

The large-scale conditions related to the LIB variability and the forcings that might have favored the warm anomalies observed in Fig. 5 were explored. Figure 6 shows the LIB-filtered geopotential height anomalies at 300 hPa and LIB-filtered OLR anomalies for the first period of the heat wave (Fig. 6e, f respectively). Also, similar fields are presented for the average of the 6 previous days (Fig. 6c, d, 9th–14th December) and the 6 days before those (Fig. 6a, b, 3rd–8th December). Between the 3rd and the 14th of December, the 12 days prior to the beginning of the heat wave, negative OLR anomalies developed over the Indian Ocean (Fig. 6b, d). In agreement, the RMM index (Wheeler and Hendon 2004) grew in amplitude and showed mostly eastward propagation along RMM MJO phase 3 (not shown). This anomalous convection may have contributed to the development of the upper-level anticyclonic anomaly to its south (Fig. 6a, c), favoring along the following days the establishment of a
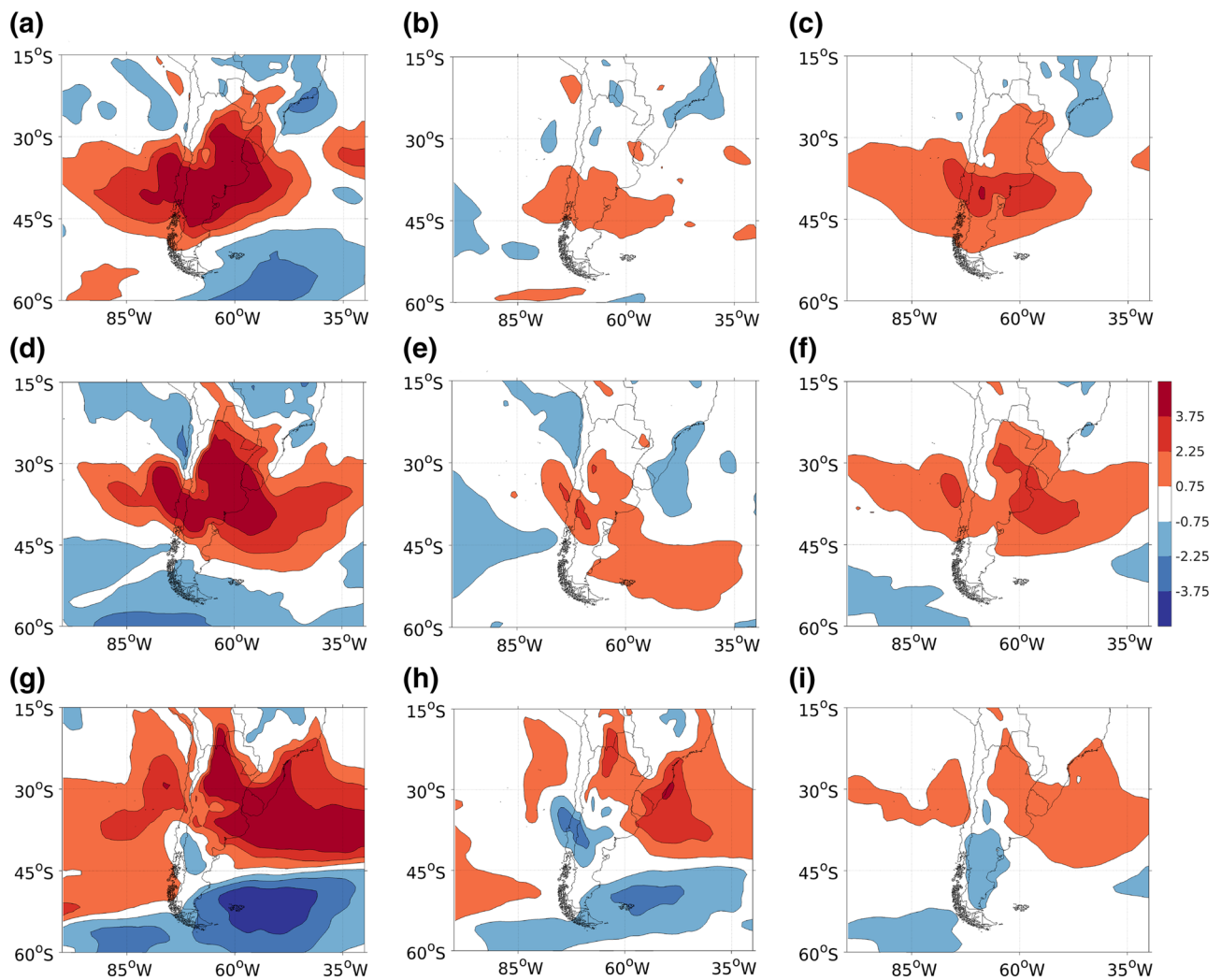
Fig. 5 **a** 925-hPa temperature anomalies, **b** SIB-filtered 925-hPa temperature anomalies and **c** LIB-filtered 925-hPa temperature anomalies for the first period of the heat wave (15–20th December). **d–f** As **a–c** but for the second period of the heat wave (21st–26th December). **g–i** As **a–c** but for the third period (27th–31st December). Units are °C

wave train which led to anticyclonic anomalies over southern South America (Fig. 6c, e). During the first period of the heat wave, the RMM MJO phase was 4 and 5, despite not showing a coherent displacement of the convective anomalies to the east (not shown).

Furthermore, from a regional perspective, the 3090-SIS pattern reflected intense activity (magnitude of the SIS index greater than one standard deviation, threshold used to define events) in the LIB variability in South America during December 2013 (Fig. 7). The index was negative since the 3rd of December, turning out in a negative event since the 11th, reaching a minimum on the 16th and lasting up to the 20th. The negative 3090-SIS related conditions can also be inferred by Fig. 6d, f, as LIB associated convection was favored in the SACZ region and inhibited over SESA. The latter also agrees with the maximum contribution of

the harmonics associated with periods between 30 and 90 days to the evolution of the temperature in Buenos Aires city (Fig. 4) during the first two periods of the heat wave. The associated regional mechanisms were pointed out by Cerne and Vera (2011), that is, a strong SACZ event generates compensatory subsidence in the subtropical region, favoring clear skies and enhancing diabatic heating. In addition, the persistent SACZ-associated circulation may have helped to geographically lock the anticyclonic anomaly in subtropical South America in the first two periods of the heat wave.

On the other hand, the temperature in Buenos Aires showed an important contribution from the SIB during the third period of the heat wave (Fig. 4), also discernible in the spatial distribution of temperature anomalies (Fig. 5h). Figure 8 shows that the 850 hPa SIB-filtered wind anomalies during this period are characterized by intense northerly
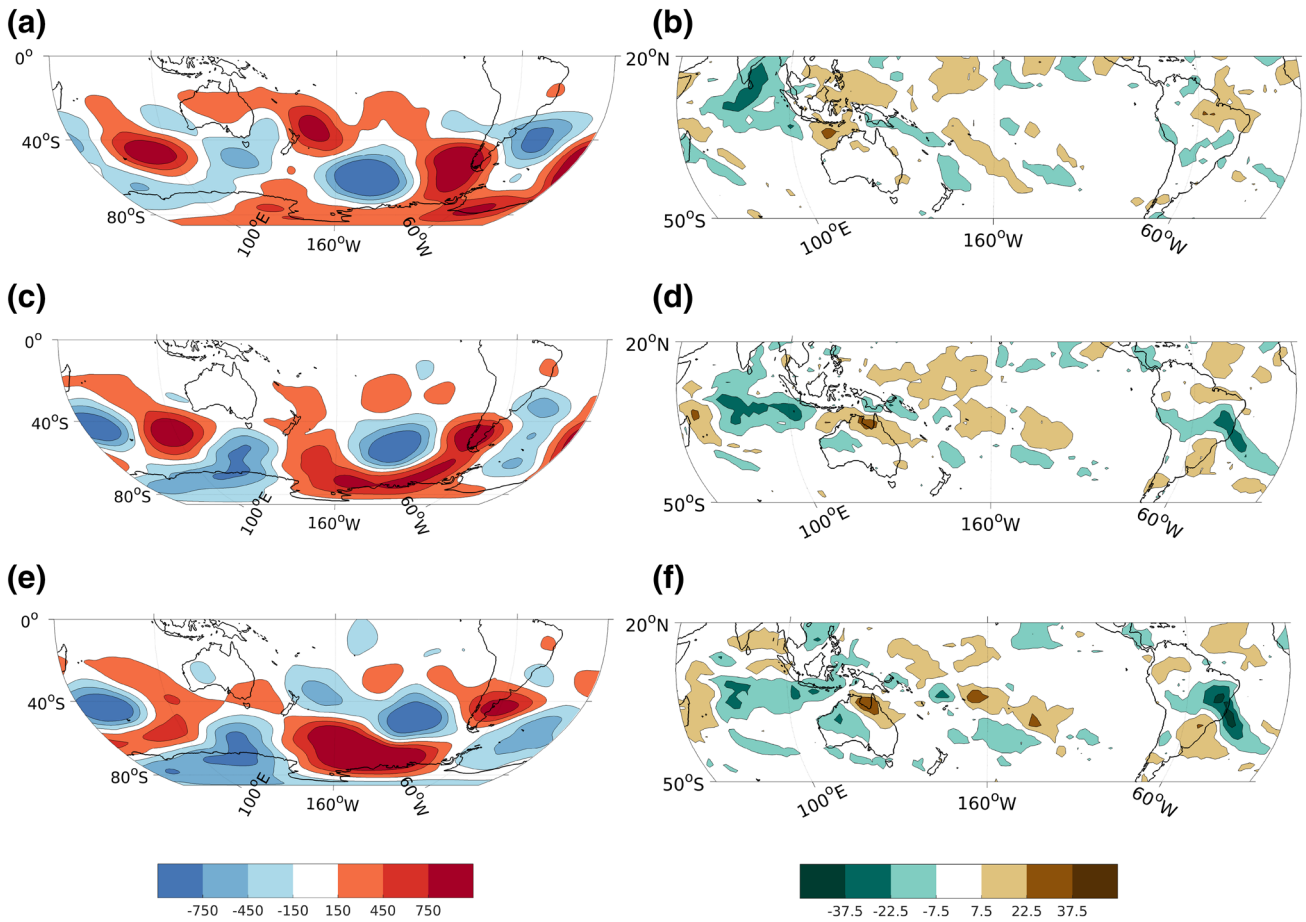
Fig. 6 LIB-filtered 300-hPa geopotential height anomalies (left column) and LIB-filtered OLR anomalies averaged between 3rd and 8th December (**a**, **b**), 9th and 14th December (**c**, **d**) and 15th and 20th December, the first period of the heat wave (15–20th December) (**e**, **f**). Units for the geopotential height anomalies are $m^2 s^{-2}$ and for OLR anomalies $W m^{-2}$
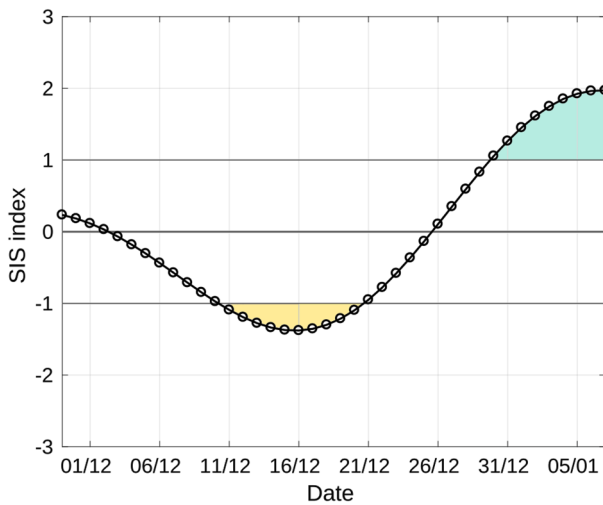

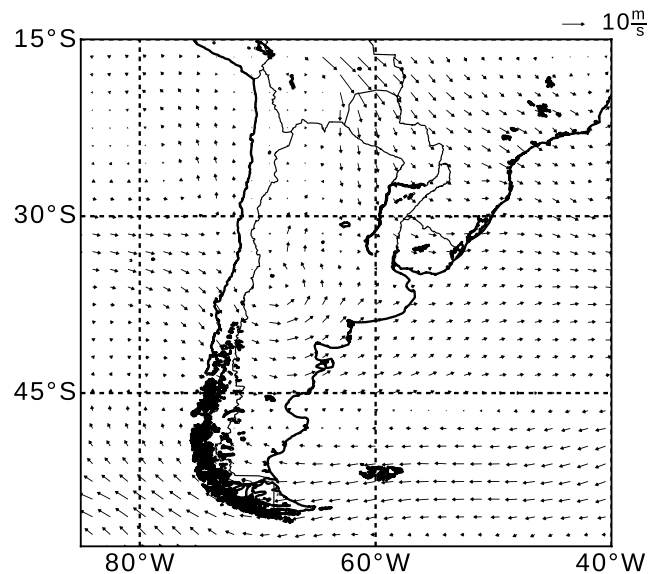**Fig. 7** 30–90 SIS index for December 2013 (standardized units)

Fig. 8 SIB-filtered 850-hPa wind anomalies averaged for the third period of the heat wave (27th–31st December)

anomalies over northern Argentina, which might have contributed to advect large temperature anomalies towards northeastern Argentina, Uruguay and southern Brazil. The contribution from the anomalous advection of warmer air from the north is a mechanism that (Cerne and Vera 2011) found to be associated to the last days of those heat waves associated to active SACZ conditions, as is this of December 2013. The maximum in temperature anomalies observed over southeastern Brazilian coastal regions (Fig. 5h) may be explained by the mechanisms recently shown by Geirinhas et al. (2019). Considering the orography of this region and the wind configuration displayed in Fig. 8, the advection of interior land masses towards the coast might have induced katabatic winds and therefore adiabatic heating, amplifying the temperature anomalies. It should be pointed out that this third period was the only period with SIB-filtered anomalies from the north, and that this direction was not observed neither in the LIB nor in the LP-filtered low-level wind anomalies in northern and central Argentina.

3.3 Low frequency forcings

The low frequency variability of temperature anomalies in Buenos Aires was also key to achieve and sustain the heat wave for 10 consecutive days, as was seen in Fig. 4. It was also pointed out that this large amplitude of the positive LP temperature anomalies only occurred 8 times between 1979 and 2014, and therefore the LP-filtered temperature anomalies, hemispheric circulation and possible forcings are analyzed in this section. Figure 9 shows the anomalies of LP-filtered temperature anomalies at 925 and of geopotential height anomalies at 300 hPa, temporally averaged over the heat wave period (15th–31st December). Positive LP-filtered temperature anomalies were observed over northern Patagonia, central and northern Argentina ranging from 0.75°C to more than 2.25°C, while negative anomalies were located over the southern tip of South America. At upper levels, positive LP-filtered geopotential height anomalies were observed over most of Argentina and Chile associated to a wave-4 pattern in midlatitudes and positive anomalies at the pole, corresponding to a negative phase of the Southern Annular Mode (SAM). LP-filtered SAM index daily values were positive between November and the 11th of December, when it changed to negative values. This negative phase of the index was associated with a downward propagation of a SAM negative phase signal that was observed until mid December in association with the seasonal breakdown of the stratospheric polar vortex (not shown). Therefore, the evolution of the hemispheric circulation anomaly patterns at extratropical and polar regions might have played a role in promoting the quasistationary conditions that regional circulation anomalies exhibited during the heat wave period.
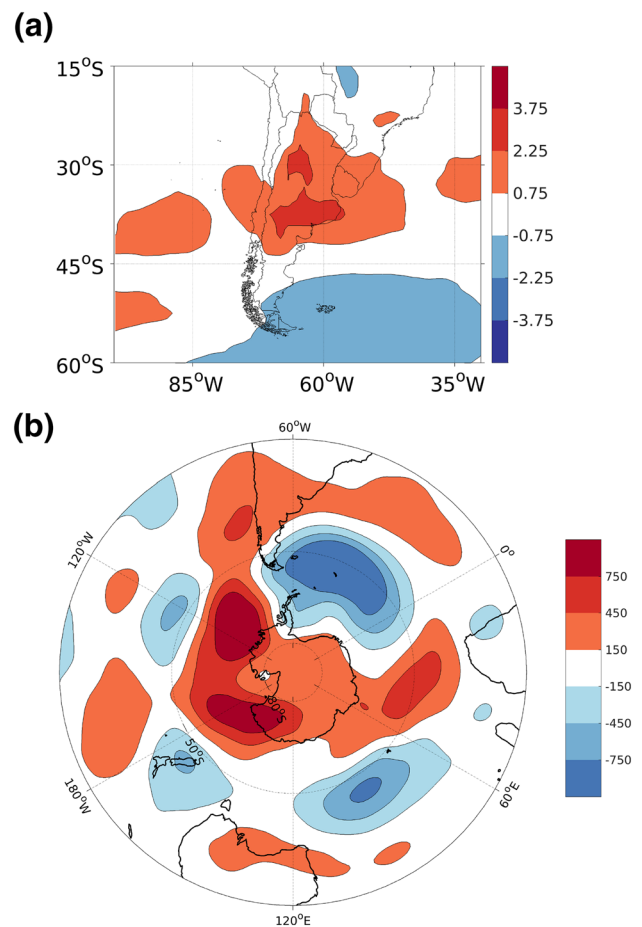
Fig. 9 **a** LB-filtered 925-hPa temperature anomalies, **b** LB-filtered 300-hPa geopotential height anomalies, averaged between 15th and 31st December 2013

There are works that suggest that preceding soil moisture conditions can affect the occurrence of hot days during the warmest months of the years (e.g. Mueller and Seneviratne 2012). In fact, for this heat wave in southern South America this relationship can be traced back to 9 months, as shown by the SSMA during the antecedent seasons of December 2013 (Fig. 10). In March–April–May (MAM) negative SSMA spanned most of the Argentine territory being particularly strong over eastern Patagonia and northern Argentina. By June–July–August (JJA) of 2013 SSMA in the northern part intensified and extended to northwestern Argentina and regions of central Argentina, while negative SSMA values over Patagonia reduced their magnitude. During September–October–November (SON) negative SSMA values remained over most of Argentina, although their magnitude was reduced due to weak but positive rainfall anomalies observed in November over eastern Argentina. Furthermore, in December the dry conditions were accentuated in the northwestern Argentina and northern Patagonia (not shown). Overall, 2013 was one of the 10 driest years observed in Argentina during the 1960–2018
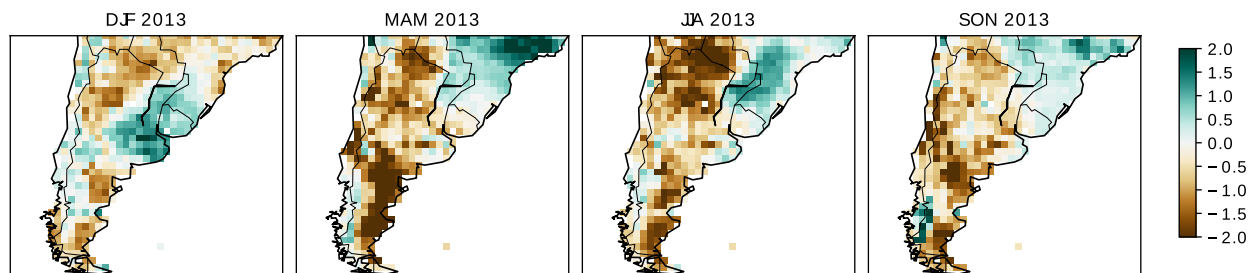
Fig. 10 Standardized soil moisture anomalies during the antecedent seasons of the December 2013 heat wave

period and therefore dry conditions were present along the seasons before the heat wave. The analysis of the circulation in the vicinity of South America (not shown) reveals that these dry conditions present throughout the austral autumn and winter were associated to positive geopotential height anomalies that promoted subsidence motions and inhibited rainfalls.

The evolution of the SSMA observed during this event was compared with that observed in a previous heat wave with similar characteristics, occurred in 2008. In this sense, in the retrospective analysis performed considering the November–March seasons of the period of 1979–2013, it was found that the heat wave occurred in November 2008, the EHF remained positive for 10 days from the 5th of November 2011 up to the 14th of the same month while the maximum amplitude recorded was similar to that for 2013 (24.59°C^2 for the event in 2008 vs 25.71°C^2 for the 2013 event). In particular, the LP temperature anomalies in the city of Buenos Aires for the 2008 event were similar to those observed fo the 2013 event (i.e. above 2°C throughout the heat wave) and the soil conditions in terms of humidity (not shown) resembled those of the event analyzed in this study (Fig. 9). The seasonal SSMA during 2008 were negative in MAM over the eastern part of Argentina, with values lower than − 2 over most of this domain (not shown). Furthermore, in JJA and SON of 2008 negative SSMA were also observed over Patagonia. Müller et al. (2014) showed that temperature anomalies during 2008 remained higher than normal during most of the year in association to rainfall deficits (precipitation was 40% up to 60% below normal over most of Argentina) and clear sky conditions. These rainfall anomalies were linked to La Niña episode observed in the first quarter of that year while the entire drought event was considered in that moment as the worst in the last 65 years (Bidegain 2009). We speculate that the dryer than normal conditions over Argentina in the antecedent seasons of both events might have favored the warm LP- filtered temperature anomalies.

4 Summary and discussion

During the second fortnight of December 2013 Buenos Aires city registered one of the longest heat waves since 1979, which also was registered in a vast region of Argentina. The excess heat indexes computed for Buenos Aires city showed that not only the mean daily temperature exceeded a statistical threshold but also that the temperature rose continuously and therefore acclimatization resulted also in heat-wave-like conditions. This heat wave occurred within the warm season with largest number of heat wave days, and it accounted for the longest consecutive period of heat wave conditions between 1979 and 2014. By disentangling the periods of variability in the temperature time series it was found that the December 2013 heat wave was the result of the combined activity of short intraseasonal (10–30 days), long intraseasonal (30–90 days) and larger (more than 90 days) time scales, and particularly occurred when the low-pass temperature series surpassed 2°C, which only occurred 8 times in the record. The synoptic variability showed little effect on the occurrence of this heat wave.

The detection of the different time scales involved in the development of the warm period led us to explore the causes that might have favored the persistence of this heat wave within each time scale. It was found that on seasonal timescales, dry soil moisture anomalies were observed in Argentina during autumn, winter and spring of 2013. Perkins et al. (2015) have shown that antecedent soil moisture exhibited a relationship with heat wave intensity over Australia, as well as Fischer et al. (2007a) and Fischer et al. (2007b) have shown for European heat waves: the depletion of soil moisture reduced latent cooling and that reduction amplified the temperature extremes during summer. Therefore, the dryer than normal conditions over Argentina in the antecedent seasons of the 2013 heat wave might be one of the causes favoring warmer anomalies. In agreement, Barrucand et al. (2014) showed using monthly data that warm and dry conditions are more frequent than cool and dry conditions in central Argentina, particularly during summertime. Moreover, in the review made by Carril et al. (2016) the authors

showed that between 1961 and 2000, warm temperature extremes during dry summers have significantly increased in the region.

The activity of the Southern Annular Mode (SAM) on the preceding seasons might also have had an influence. Negative phase of the SAM was observed during the event that resulted from a downward propagation of the signal from the stratosphere to the troposphere, in association to the polar vortex breakdown that took place in November. Further work needs to be done to assess the role that the SAM might play promoting the large scale conditions that favor the occurrence of this type of heat waves.

In addition, clear evidences were found about the role played by the intraseasonal variability in the persistence of the heat wave. The development of an MJO event over the Indian Ocean (RMM phase 3) 12 days prior to the beginning of the heat wave seems to have helped organizing the extratropical wave train that build up the anticyclonic upper-level anomalies over southern South America observed in the long intraseasonal time scale. Furthermore, a negative 3090-SIS event centered in the 20th December revealed the intensity of the active SACZ during the first 12 days of the heat wave, while during the last days it was the northerly advection of warmer air in the 10–30-day time scale that maintained the intensity of the temperature anomalies. This combination of intensified SACZ activity, which generates clear skies and diabatic heating in the subtropics, and subsequent northerly advection was the mechanism described in Cerne and Vera (2011) for intraseasonally-modulated heat waves. The key role of the intraseasonal variability is suspected to have influenced the moderate skill of forecast of this heat wave for ranges beyond the weather, as was found by Osman and Alvarez (2018) using two models of the S2S Project database (Vitart et al. 2017).

Finally, it is worth to mention that Hannart et al. (2015) showed that anthropogenically-forced global warming was a necessary condition for the development of this heatwave. Moreover, the climate forcing associated with anthropogenic greenhouse gas increase have increased the risk of an event like this one by a factor of five. In agreement, it has been recently assessed that human-induced global warming has already caused more frequent heatwaves in most of land regions, and in particular urban heat islands often amplify their impacts in cities (Hoegh-Guldberg et al. 2018). In addition, future climate change projections confirm that the health of people living within urbanized areas will be affected by an increase exposure to extreme thermal conditions (e.g. Dereczynski et al. 2013). Zhao et al. (2018) discussed the geospatial synergistic interaction between the urban heat island effect and heat waves for cities in different climate regions for present and future warmer climates, and show that heat waves produce an additional effect of increased heat stress in cities associated with the lack of surface moisture in urban areas and the low wind speed conditions. Therefore, it will be important that future studies address the combined influence of the natural climate variability and the human-induced climate change on the heat waves like the one studied here. This knowledge will be important for example, for the development of city adaptation plans.

References

Alessandro AP, de Garín AB (2003) A study on predictability of human physiological strain in Buenos Aires City. Meteorol Appl 10(3):263–271

Almeira G, Rusticucci M, Suaya M (2016) Relación entre mortalidad y temperaturas extremas en buenos aires y rosario. Meteorologica 41(2):65–79

Alvarez MS, Vera CS, Kiladis GN (2017) MJO modulating the activity of the leading mode of intraseasonal variability in south America. Atmosphere 8(12):232

Barros VR, Boninsegna JA, Camilloni IA, Chidiak M, Magrín GO, Rusticucci M (2015) Climate change in argentina: trends, projections, impacts and adaptation. Wiley Interdiscip Rev Clim Change 6(2):151–169

Barrucand M, Vargas W, Bettolli ML (2014) Warm and cold dry months and associated circulation in the humid and semi-humid argentine region. Meteorol Atmos Phys 123(3):143–154

Bastos A, Gouveia CM, Trigo RM, Running SW (2014) Analysing the spatio-temporal impacts of the 2003 and 2010 extreme heatwaves on plant productivity in europe. Biogeosciences 11(13):3421–3435

Berrisford P, Dee D, Poli P, Brugge R, Fielding K, Fuentes M, Kållberg P, Kobayashi S, Uppala S, Simmons A (2011) The era-interim archive version 2.0. Shinfield Park, Reading

Bidegain M (2009) Severe drought in central Argentina and Uruguay. In: Peterson TC, Baringer MO (eds) State of the climate in 2008, chapter 7, vol 90. American Meteorological Society, Boston, p S138

Campetella C, Rusticucci M (1998) Synoptic analysis of an extreme heat wave over argentina in March 1980. Meteorol Appl 5(3):217–226

Carril AF, Cavalcanti I, Menéndez C, Sörensson A, López-Franca N, Rivera J, Robledo F, Zaninelli P, Ambrizzi T, Penalba O, da Rocha R, Sánchez E, Bettolli M, Pessacg N, Renom M, Ruscica R, Solman S, Tencer B, Grimm A, Rusticucci M, Cherchi A, Tedeschi R, Zamboni L (2016) Extreme events in the la plata basin: a retrospective analysis of what we have learned during claris-lpb project. Clim Res 68:95–116

Cerne SB, Vera CS (2011) Influence of the intraseasonal variability on heat waves in subtropical South America. Clim Dyn 36(11):2265–2277

Cerne SB, Vera CS, Liebmann B (2007) The nature of a heat wave in eastern Argentina occurring during salljex. Mon Weather Rev 135(3):1165–1174

Dereczynski C, Luiz Silva W, Marengo J (2013) Detection and projections of climate change in Rio de Janeiro, Brazil. Am J Clim Change 2(1):25–33

Duchon CE (1979) Lanczos filtering in one and two dimensions. J Appl Meteorol 18(8):1016–1022

Ek MB, Mitchell KE, Lin Y, Rogers E, Grunmann P, Koren V, Gayno G, Tarpley JD (2003) Implementation of Noah land surface model advances in the national centers for environmental prediction operational mesoscale eta model. J Geophys Res Atmos 108(D22):8851

Fischer EM, Seneviratne SI, Lüthi D, Schär C (2007a) Contribution of land-atmosphere coupling to recent European summer heat waves. Geophys Res Lett 34(6):L06707

Fischer EM, Seneviratne SI, Vidale PL, Lüthi D, Schär C (2007b) Soil moisture–atmosphere interactions during the 2003 European summer heat wave. J Clim 20(20):5081–5099

García-Herrera R, Díaz J, Trigo RM, Luterbacher J, Fischer EM (2010) A review of the European summer heat wave of 2003. Crit Rev Environ Sci Technol 40(4):267–306

Geirinhas JL, Trigo RM, Libonati R, Castro LC, Sousa PM, Coelho CA, Peres LF, de Avelar FM, Magalhães M (2019) Characterizing the atmospheric conditions during the 2010 heatwave in Rio de Janeiro marked by excessive mortality rates. Sci Total Environ 650:796–808

Gonzalez PLM, Vera CS (2014) Summer precipitation variability over South America on long and short intraseasonal timescales. Clim Dyn 43(7):1993–2007

Hannart A, Vera C, Cerne B, Otto FEL (2015) Causal influence of anthropogenic forcings on the argentinian heat wave of December 2013. Bull Am Meteorol Soc 96(12):S41–S45

Hoegh-Guldberg O, Jacob D, Taylor M, Bindi M, Brown S, Camilloni I, Diedhiou A, Djalante R, Ebi KL, Engelbrecht F, Guiot J, Hijioka Y, Mehrotra S, Payne A, Seneviratne SI, Thomas A, Warren R, Zhou G (2018) Impacts of 1.5 c global warming on natural and human systems. In: Masson-Delmotte V, Zhai P, Portner HO, Roberts D, Skea J, Shukla PR, Pirani A, Moufouma-Okia W, Péan C, Pidcock R, Connors S, Matthews JBR, Chen Y, Zhou X, Gomis MI, Lonnoy E, Maycock T, Tignor MTW (eds) Global Warming of 1.5 C. An IPCC special report on the impacts of global warming of 1.5 C above pre-industrial levels and related global greenhouse gas emission pathways, in the context of strengthening the global response to the threat of climate change, sustainable development, and efforts to eradicate poverty, chapter 3, pp 175–311 **(in press)**

Leva P, García M, Veles M, Valtorta S (2005) Ganado lechero en la cuenca central de Santa Fe-Córdoba: efecto del estrés estival e impacto esperado del cambio global. FAVE 14(1):39–48. https://doi.org/10.14409/fave.v14i1.3084

Madden RA, Julian PR (1994) Observations of the 40–50-day tropical oscillation: a review. Mon Weather Rev 122(5):814–837

Mueller B, Seneviratne SI (2012) Hot days induced by precipitation deficits at the global scale. Proc Natl Acad Sci 109(31):12398–12403

Müller OV, Berbery EH, Alcaraz-Segura D, Ek MB (2014) Regional model simulations of the 2008 drought in southern south america using a consistent set of land surface properties. J Clim 27(17):6754–6778

Nogues-Paegle J, Mo KC (1997) Alternating wet and dry conditions over South America during summer. Monthly Weather Review 125(2):279–291

Osman M, Alvarez MS (2018) Subseasonal prediction of the heat wave of december 2013 in southern South America by the poama and bcc-cps models. Clim Dyn 50(1):67–81

Perkins SE, Alexander LV (2013) On the measurement of heat waves. J Clim 26(13):4500–4517

Perkins SE, Argüeso D, White CJ (2015) Relationships between climate variability, soil moisture, and australian heatwaves. J Geophys Res Atmos 120(16):8144–8164 2015JD023592

Rodell M, Houser PR, Jambor U, Gottschalck J, Mitchell K, Meng C-J, Arsenault K, Cosgrove B, Radakovich J, Bosilovich M, Entin JK, Walker JP, Lohmann D, Toll D (2004) The global land data assimilation system. Bull Am Meteorol Soc 85(3):381–394

Ruscica RC, Sörensson AA, Menéndez CG (2015) Pathways between soil moisture and precipitation in southeastern South America. Atmos Sci Lett 16(3):267–272

SMN (2014) Informe especial debido a la ocurrencia de una ola decalor excepcional en Argentina durante Diciembre de 2013. Technical report, Servicio Meteorológico Nacional

Spennemann PC, Rivera JA, Saulo AC, Penalba OC (2015) A comparison of gldas soil moisture anomalies against standardized precipitation index and multisatellite estimations over South America. J Hydrometeorol 16(1):158–171

Vera CS, Alvarez MS, Gonzalez PLM, Liebmann B, Kiladis GN (2018) Seasonal cycle of precipitation variability in south America on intraseasonal timescales. Clim Dyn 51(5):1991–2001. https://doi.org/10.1007/s00382-017-3994-1

Vitart F, Ardilouze C, Bonet A, Brookshaw A, Chen M, Codorean C, Déqué M, Ferranti L, Fucile E, Fuentes M, Hendon H, Hodgson J, Kang H-S, Kumar A, Lin H, Liu G, Liu X, Malguzzi P, Mallas I, Manoussakis M, Mastrangelo D, MacLachlan C, McLean P, Minami A, Mladek R, Nakazawa T, Najm S, Nie Y, Rixen M, Robertson AW, Ruti P, Sun C, Takaya Y, Tolstykh M, Venuti F, Waliser D, Woolnough S, Wu T, Won D-J, Xiao H, Zaripov R, Zhang L (2017) The subseasonal to seasonal (s2s) prediction project database. Bull Am Meteorol Soc 98(1):163–173

Wheeler MC, Hendon HH (2004) An all-season real-time multivariate MJO index: development of an index for monitoring and prediction. Mon Weather Rev 132(8):1917–1932

Zhao L, Oppenheimer M, Zhu Q, Baldwin JW, Ebi KL, Bou-Zeid E, Guan K, Liu X (2018) Interactions between urban heat islands and heat waves. Environ Res Lett 13(3):034003